

# STEADY STATE SOLUTION OF MAGNETOHYDRODYNAMICS (MHD) FREE CONVECTION HEAT AND MASS TRANSFER IN AN ANNULUS WITH CONVECTIVE BOUNDARY CONDITIONS OF MIXED KIND

Isah Bala Yabo and Muhammad Murtala Hamza

<sup>1</sup>*Bashiru Abdullahi Department of Mathematics and Statistics  
Abdu Gusau Polytechnic, Talata, Mafara*

<sup>2</sup>*Department of Mathematics Usman Danfodio University, Sokoto*

## Abstract

The problem considered is the steady flow of an electrically conducting, incompressible fluid, in the annular space between two infinitely long circular cylinders, under a radially impressed magnetic field with convective boundary conditions of mixed kind. The general Magnetohydrodynamics equations are simplified by the conditions of the problem to two equations in velocity and temperature. The Rosseland approximation is applied to describe the radiative heat flux in the energy equation where the magnetic field is incorporated in the momentum equation. Due to nonlinearity of the model in the presence of radiative parameter, the solution of the differential equation that described the flow was solved using Perturbation method. The velocity, the temperature, Skin friction and Nusselt number are obtained and their behaviors are discussed with help of line graph. The results obtained show that the flow is significantly been influence by the fluid flow parameters.

**Keywords:** *Magnetohydrodynamics, Steady state, heat transfer, Annulus, convective boundary conditions.*

## 1.0 Introduction

Convective heat transfer in horizontal annuli has attracted many attentions in engineering sciences due to its wide applications such as in solar collector–receiver, vapor condenser for water distillation and food process, construction of electrical motors and generators, cooling of electronic components, nuclear reactors, thermal storage systems, heating and cooling of underground electric cables, completion of oil source and aircraft fuselage insulation. Ho *et al* (1988) conducted a research on natural convection in concentric and eccentric horizontal cylindrical annuli with mixed boundary conditions. Kumar 1988 studied natural convection of gas in a horizontal annulus, where the inner cylinder is heated by the application of a constant heat flux and the outer cylinder is isothermally cooled. Tsui and Tremblay (2000) conducted a research on transient natural convection heat transfer problem between two horizontal isothermal cylinders formed within the Boussinesqs approximation and solved numerically through the vorticity-stream function approach. Numerical prediction of natural convection heat transfer in horizontal annulus where the inner cylinder is hotter than outer was conducted by Date (1986) Yoo (1990) conducted research on natural convection in a narrow horizontal cylindrical annulus for fluid of  $Pr \leq 0.3$  been investigated. Mizushima *et al* (2001) investigated transition of natural convection in an annulus between horizontal concentric cylinders theoretically by assuming two-dimensional and incompressible flow fields. Shah *et al* (2011) investigated the effect of Nano

fluid on the natural convection heat transfer and fluid flow through an annular tube with an inner heat generating solid circular rod. Yoo 1999 in his paper, discussed the existence of dual solution and role of Prandtl number on bifurcation. Adachi and Imai (2007) performed three-dimensional linear stability analysis of air in horizontal concentric annuli between concentric cylinders by using a spectral method. Chen and Hsu (2007) conducted a research on finite difference method in conjunction with least-squares scheme and experimental temperature data is used to predict the average heat transfer coefficient and fin efficiency on the fin of annular-fined tube. Heat transfer characteristics of Taylor-Couette- Poiseuille flow in an annular channel by mounting longitudinal ribs on the rotating inner cylinder was discussed by Jeng et al (2007). Cienfrini *et al* (2011) compiled a comprehensive theoretical study on natural convection heat transfer in Nano fluid contained inside the horizontal annular space existing between two long concentric cylinder whose surface are maintained at different uniform temperatures, with primary scope to determine the main heat transfer features for various operating conditions, Nano particle diameters, and solid-liquid combination. Alawadi (2008) investigated natural convection flow in a horizontal annulus enclosure with a transversely oscillating inner cylinder. Yeh (2002) examined a numerical solution on horizontal concentric annulus with open ends and conditions of either adiabatic or isothermal outer cylinder surface. Yoo (2003) investigated that, dual steady state solutions exist above a critical Rayleigh number for free convective flows in a horizontal annulus with constant heat-flux wall. Soleiman *et al* (2012) conducted a numerical investigation of natural convection heat transfer in a semi-annulus enclosure filled with Nano fluid using the control volume based finite element method. Tahir and Mital (2012) developed and tested a discrete phase model for forced convection of Nano fluid in a circular tube subjected to a uniform heat flux. Sheikholeslami et al (2012) and Sheikholeslami *et al* (2013) examined the role of magnetic field on natural convection flow of Nano-fluid using Lattice Boltzmann method. Ashorynejadeed *et al* (2013) conducted an investigation on effect of static radial magnetic field on natural convection heat transfer in a horizontal cylindrical annulus enclosure filled with Nano fluid using Boltzmann.

Habibi and Pop (2013) studied numerically natural convection flow and heat transfer of Copper water Nano fluid inside eccentric horizontal annulus while the inner and outer cylinder are kept at constant temperatures. Steady-state problem of a magnetic fluid filling a porous annulus between two cylindrical walls under the influence of a non-uniform radially outward magnetic field has been investigated by Shihhao *et al* (2014). They examined the effect of the strength of the externally applied magnetic field, the permeability of the porous annulus, and the conductivity of the cylindrical walls through the angular velocity components, as well as the induced magnetic field. Jha *et al* (2017) investigated both analytically and numerically the interaction of fully developed natural convection flow with thermal radiation inside vertical annulus.

## 2.0 Mathematical formulation

The physical problem under consideration consists of a transient natural convection flow in an infinite vertical annulus formed by two infinite concentric vertical cylinders in presence of thermal radiation. The transient flow formation is due to sudden heating of outer surface of inner cylinder in presence of thermal radiation. The physical properties of the working fluid are assumed to be constant. A schematic diagram of the present problem is shown in Figure 1. At time  $t' \leq 0$ , both the fluid and cylinder are assumed to be at the same temperature  $T_0$  with absence of fluid motion. At time  $t' > 0$ , the temperature of the outer surface of inner cylinder at  $r = a^*$  is suddenly raised to  $T_w$  ( $T_w > T_0$ ) causing transient free convection current. Since the flow is fully developed and the cylinders are of infinite length, the flow depends on radial coordinate ( $r'$ ) and time ( $t'$ ). Using of Boussinesq's approximation, the governing equations in dimensional form are

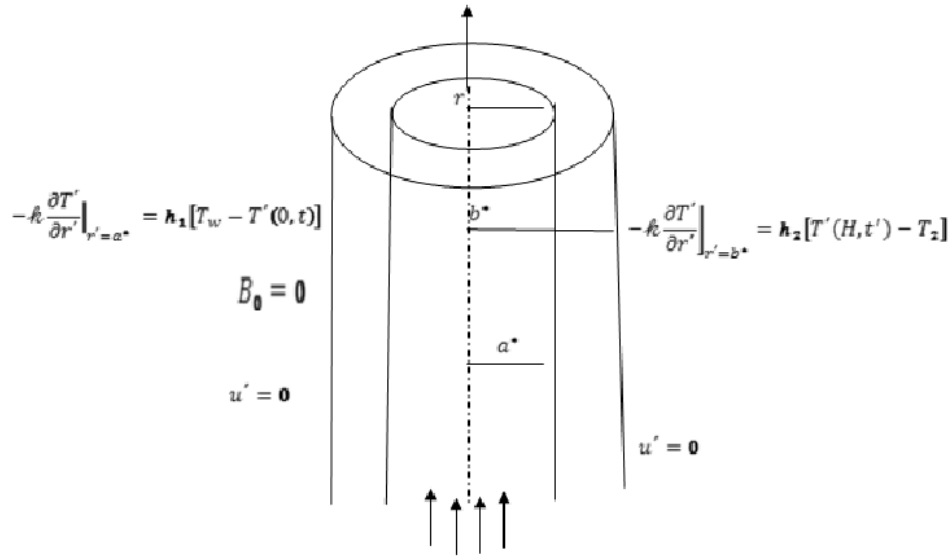


Figure 1: Geometry of the problem

$$\frac{\partial u'}{\partial t'} = \frac{\gamma}{r'} \frac{\partial}{\partial r'} \left( r' \frac{\partial u'}{\partial r'} \right) + g\beta(T' - T_0) \quad (1)$$

$$\frac{\partial T'}{\partial t'} = \alpha \left[ \frac{1}{r'} \frac{\partial}{\partial r'} \left( \frac{\partial T'}{\partial r'} \right) - \frac{1}{K} \frac{\partial q_r}{\partial r'} \right] \quad (2)$$

Where  $\alpha$  is the thermal diffusivity,  $K$  is the thermal conductivity,  $\beta$  is the coefficient of the thermal expansion,  $\sigma$  is the fluid electrical conductivity,  $g$  is the gravitational acceleration and  $B_0$  is the strength of applied magnetic field. The quantity  $q_r$  appearing on the right hand side of Equation (2) represents the radiative heat flux in the  $r'$ - direction.

Initial and boundary conditions:

$$\left. \begin{aligned} t' \leq 0: \quad u' = 0; \quad T' = T_0 \text{ for } a^* \leq r' \leq b^* \\ t' > 0: \quad u' = 0, -k \frac{\partial T'}{\partial r'} \Big|_{r'=a^*} = h_1 [T_w - T'(0, t)] \\ t' > 0: u' = 0, \quad -k \frac{\partial T'}{\partial r'} \Big|_{r'=b^*} = h_2 [T'(H, t') - T_2] \end{aligned} \right\} \quad (3)$$

The radiation heat flux term in the problem is simplified by using the Rosseland approximation

$$q_r = \frac{-4\sigma\partial T'^4}{3k\partial r'} \quad (4)$$

To obtain the non-dimensional form of the above equations, the following dimensionless Variables are introduced.

$$\begin{aligned} t = \frac{t'\gamma}{\alpha^{*2}}, \quad r = \frac{r'}{a^*}, \quad P_r = \frac{\gamma}{\alpha}, \quad \theta = \frac{T' - T_0}{T_w - T_0}, B_{i1} = \frac{h_1 a^*}{\gamma}, B_{i2} = \frac{h_2 a^*}{\gamma}, \\ rt = \frac{T_2 - T_0}{T_w - T_0}, \lambda = \frac{b^*}{a^*}, u = u' \gamma [g\beta a^{*2} (T_w - T_0)]^{-1}, \end{aligned} \quad (5)$$

$$\text{Where } R = \frac{4\sigma(T_1 - T_0)^3}{Kk}, C_T = \frac{T_0}{T_w - T_0} \quad (6)$$

Using Equations (4) to (6) in Equations (1) and (2), we obtain the following dimensionless equations for velocity and temperature respectively.

$$\frac{\partial u}{\partial t} = \frac{1}{r} \frac{\partial}{\partial r} \left( r \frac{\partial u}{\partial r} \right) + \theta \quad (7)$$

$$P_r \frac{\partial \theta}{\partial t} = \left[ 1 + \frac{4R}{3} (C_T + \theta)^2 \right] \frac{1}{r} \frac{\partial}{\partial r} \left( r \frac{\partial \theta}{\partial r} \right) + 4R [C_T + \theta]^2 \left( \frac{\partial \theta}{\partial r} \right)^2 \quad (8)$$

New boundary conditions:

$$\left. \begin{aligned} t \leq 0: \quad \text{at } r = 1, u = 0, \theta = 0 \text{ at } 1 \leq r \leq \lambda \\ t > 0: \quad \left\{ \begin{aligned} -\frac{\partial \theta}{\partial r} \Big|_{r=1} &= B_{i1} [1 - \theta] \\ -\frac{\partial \theta}{\partial r} \Big|_{r=\lambda} &= B_{i2} [\theta - rt] \end{aligned} \right. \quad u = 0 \end{aligned} \right\} \quad (9)$$

### 3 Analytical Solution

Equations (7) and (8) are highly non-linear such that analytical solution can't be obtained. Hence

one can obtain its steady state solution using perturbation method by putting  $\frac{\partial u}{\partial t} = \frac{\partial \theta}{\partial t} = 0$

$$\frac{1}{r} \frac{d}{dr} \left( r \frac{du}{dr} \right) + \theta = 0 \quad (10)$$

$$\left[ 1 + \frac{4R}{3} (C_T + \theta)^2 \right] \frac{1}{r} \frac{d}{dr} \left( r \frac{d\theta}{dr} \right) + 4R [C_T + \theta]^2 \left( \frac{d\theta}{dr} \right)^2 = 0 \quad (11)$$

The solution to the dimensionless set of ordinary differential equations in (10) and (11) can be obtained by representing velocity and temperature as follows:

$$u(r) = u_0(r) + Ru_1(r) + \dots + \sum_{j=0}^{\infty} R^j u_j(r) \quad (12)$$

$$\theta(r) = \theta_0(r) + R\theta_1(r) + \dots + \sum_{j=0}^{\infty} R^j \theta_j(r) \quad (13)$$

Substituting equation (12) and (13) into equation (10) and (11) respectively and equating like powers of R, one obtains the harmonic and non-harmonic boundary value problem for  $j = 0$  and  $j = 1$  as:

$$\frac{1}{r} \frac{d}{dr} \left( r \frac{du_0}{dr} \right) + \theta_0 = 0 \quad (14)$$

$$\frac{1}{r} \frac{d}{dr} \left( r \frac{du_1}{dr} \right) + \theta_1 = 0 \quad (15)$$

$$\frac{1}{r} \frac{d}{dr} \left( r \frac{d\theta_0}{dr} \right) = 0 \quad (16)$$

$$\frac{1}{r} \frac{d}{dr} \left( r \frac{d\theta_1}{dr} \right) + \frac{4}{3} (C_T + \theta_0)^2 \frac{1}{r} \frac{d}{dr} \left( r \frac{d\theta_0}{dr} \right) + 4 [C_T + \theta_0]^2 \left( \frac{d\theta_0}{dr} \right)^2 = 0 \quad (17)$$

Subject to the following boundary conditions

$$\left. \begin{array}{l} t \leq 0: \quad \text{at } r = 1, u = 0, \theta = 0 \text{ at } 1 \leq r \leq \lambda \\ t \geq 0: \quad \left\{ \begin{array}{l} u = 0, \left[ \begin{array}{l} \frac{d\theta_0}{dr} = B_{i1} [(1 - \theta_0)_0], \quad -\frac{d\theta_1}{dr} = B_{i1} \theta_0 \text{ (at } r = 1) \\ \frac{d\theta_0}{dr} = B_{i2} (\theta_0 - rt), \quad \frac{d\theta_1}{dr} = B_{i2} \theta_1 \text{ (at } r = \lambda) \end{array} \right. \end{array} \right\} \quad (18)$$

The values of  $\varphi_0$  and  $\varphi_1$  from (16) and (17) using the boundary condition (18) are:

$$\theta_0 = A_1 \log r + A_2 \quad (19)$$

$$\theta_1 = K_1 \frac{(\log r)^2}{2} + K_2 \frac{(\log r)^3}{6} + K_3 \frac{(\log r)^4}{12} + K_4 \log r + K_5 \quad (20)$$

Since equation (14) and (15) are coupled with  $\theta_0(r)$  and  $\theta_1(r)$ , using result obtained in equation (19) and (20), the solutions of  $u_0(r)$  and  $u_1(r)$  are:

$$u_0(r) = A_1 \frac{r^2}{4} - A_1 \frac{r^2 \log r}{4} - A_2 \frac{r^2}{4} + C_1 \log r + C_2 \quad (21)$$

$$u_1(r) = H_1 r^2 (\log[r]^4) - H_2 r^2 (\log r)^3 - H_3 r^2 (\log r)^2 + H_4 r^2 \log r - H_5 r^2 + G_1 \log r + G_2 \quad (22)$$

The complete solutions of velocity, temperature, Skin friction and Nusselt number equations are:

**Velocity equation:**

$$u(r) = A_1 \frac{r^2}{4} - A_1 \frac{r^2 \log r}{4} - A_2 \frac{r^2}{4} + C_1 \log r + C_2 + R(H_1 r^2 (\log r)^4 - H_2 r^2 (\log r)^3 - H_3 r^2 (\log r)^2 + H_4 r^2 \log r - H_5 r^2 + G_1 \log r + G_2)$$

**Temperature equation:**

$$\theta(r) = A_1 \log r + A_2 + R \left( K_1 \frac{(\log r)^2}{2} + K_2 \frac{(\log r)^3}{6} + K_3 \frac{(\log r)^4}{12} + K_4 \log r + K_5 \right)$$

**Skin friction**

$$\tau_0 = \left. \frac{du}{dr} \right|_{r=1} = \frac{A_1}{4} - \frac{A_2}{2} + C_1 + RH_4 - 2RH_5 + RG_1$$

$$\tau_1 = \left. \frac{du}{dr} \right|_{r=\lambda} = \frac{A_1 \lambda}{4} - \frac{A_1 \lambda \log \lambda}{2} - \frac{A_2 \lambda}{2} + \frac{c_1}{\lambda} + 4RH_1 \lambda (\log \lambda)^3 + 2RH_1 \lambda (\log \lambda)^4 - 3RH_2 \lambda (\log \lambda)^2 - 2RH_2 \lambda (\log \lambda)^3 - 2RH_3 \lambda \log \lambda - 2RH_3 \lambda (\log \lambda)^2 + RH_4 \lambda \log \lambda - 2R\lambda H_5 + \frac{RG_1}{\lambda}$$

**Nusselt number**

$$Nu_0 = \left. \frac{d\theta}{dr} \right|_{r=1} = A_1 + RK_4$$

$$Nu_1 = \left. \frac{d\theta}{dr} \right|_{r=\lambda} = \frac{A_1}{\lambda} + \frac{RK_1 \log \lambda}{\lambda} + \frac{RK_1 (\log[\lambda]^2)}{2\lambda} + \frac{RK_2 (\log[\lambda]^3)}{3\lambda} + \frac{RK_4}{\lambda}$$

#### 4.0 Results

The paper examined the free-convective steady-state MHD flow restricted through an annulus with boundary condition of mixed kind. The system of governing equations of the physical situation presented in (10) and (11) is solved using the Perturbation method. The result that clearly reports the influence of the flow governing parameters on velocity, temperature, skin friction and Nusselt number has been shown graphically in Figures 2 to Figure 23.

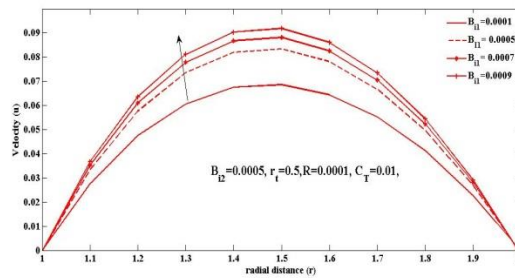


Figure 2: velocity profile with different values of Biot number

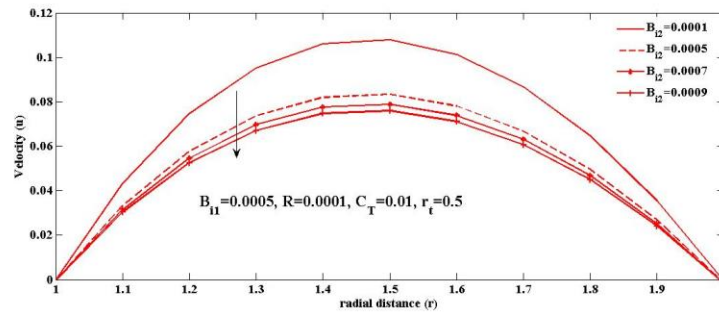


Figure 3: velocity profile for different values of Biot number

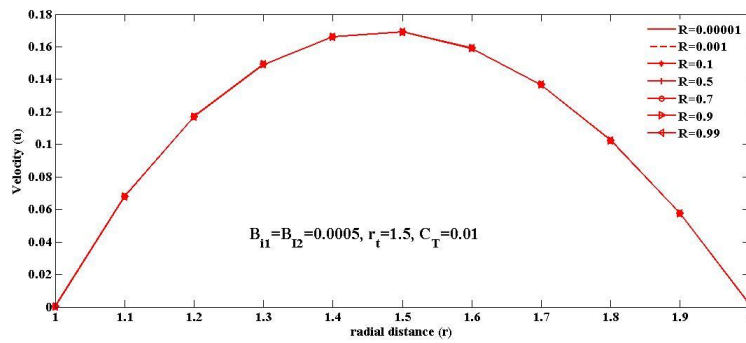


Figure 4: velocity profile for different values of R

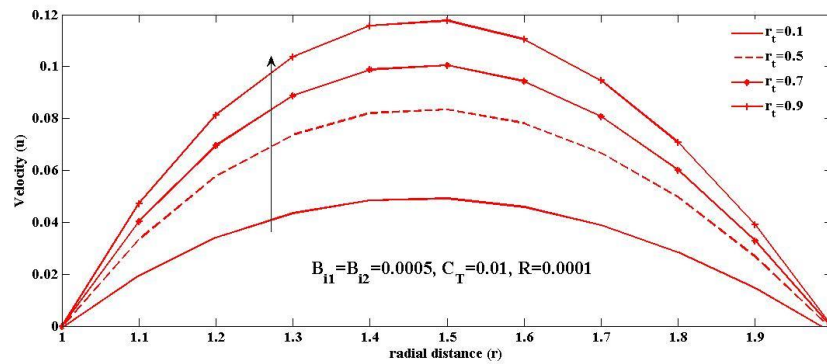


Figure 5: velocity profile for different values of  $r_t$

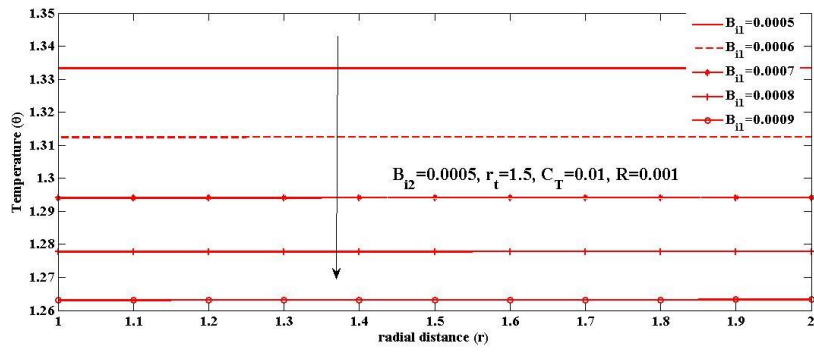


Figure 6: Temperature profile for different values of  $B_{I1}$

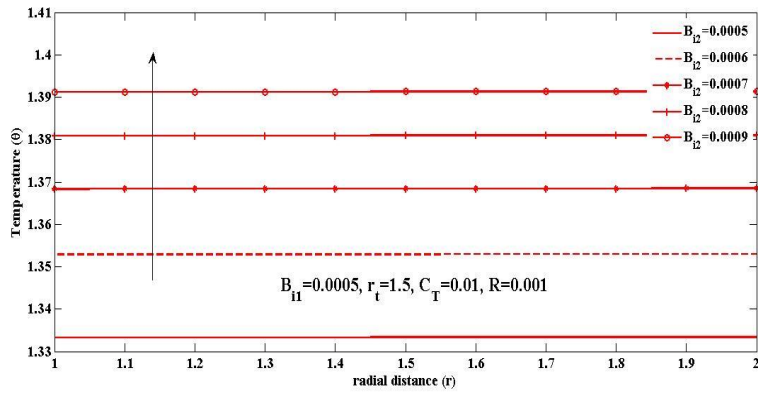
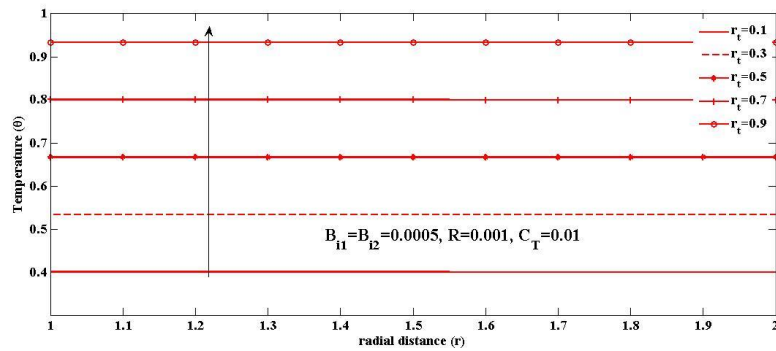
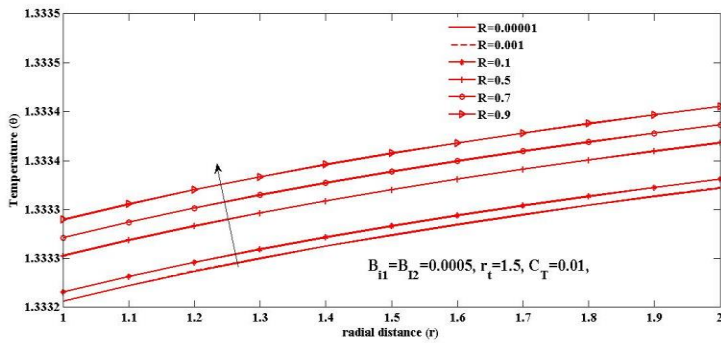
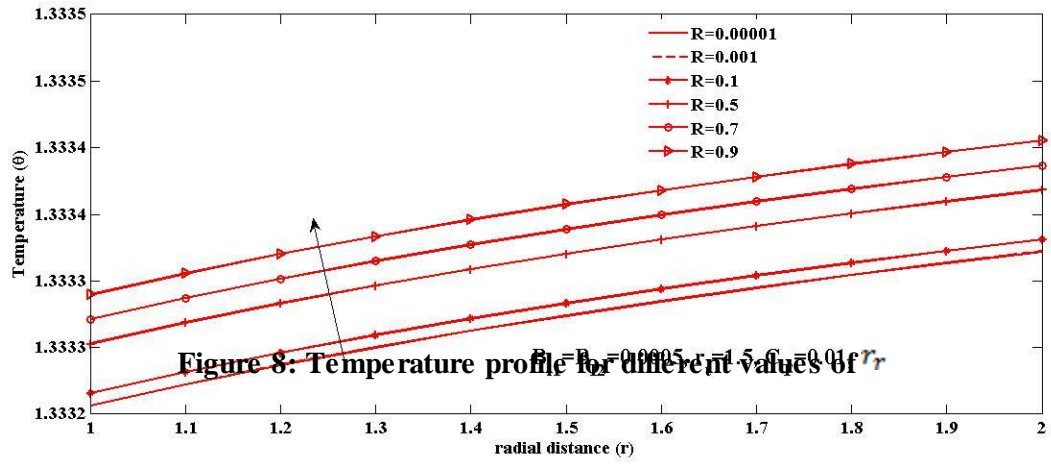


Figure 7: Temperature profile for different values of  $B_{I2}$







**Figure 9: Temperature profile for different values of  $R$**

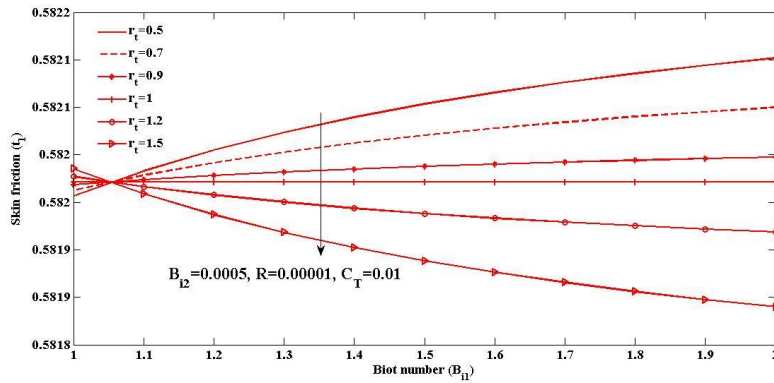


Figure 10: Skin friction profile at  $r = 1$  for different values of  $r_t$

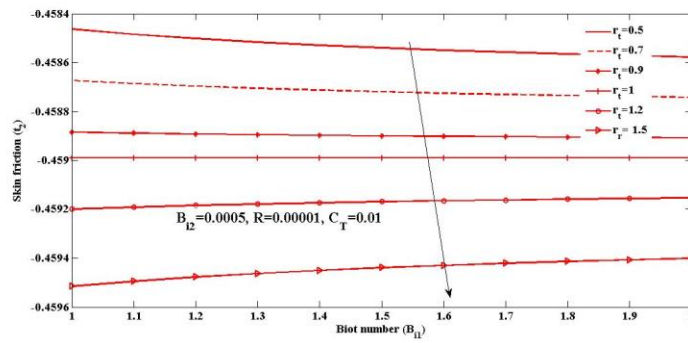


Figure 11: Skin friction profile at  $r = \lambda$  for different values of  $r_t$

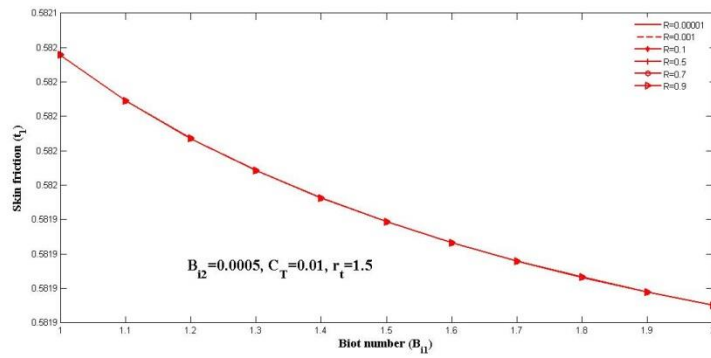


Figure 12: Skin friction profile at  $r = 1$  for different values of  $R$

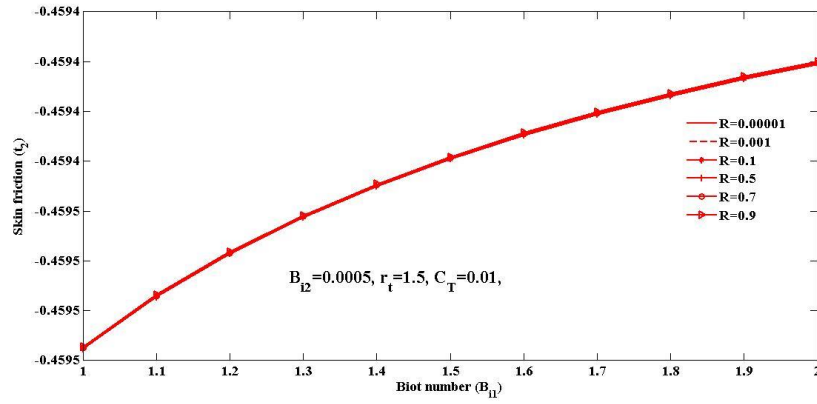


Figure 13: Skin friction profile at  $r = \lambda$  for different values of  $R$

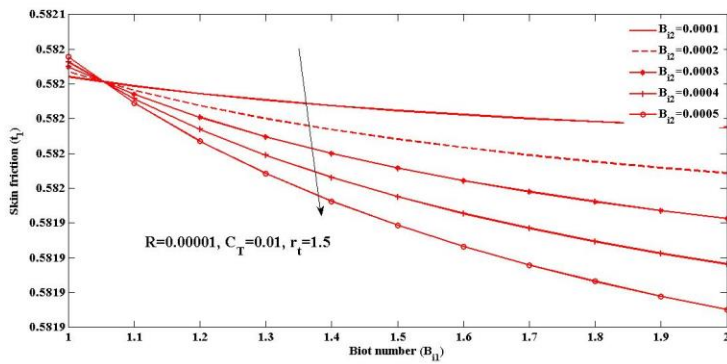


Figure 14: Skin friction profile at  $r = 1$  for different values of  $B_{12}$

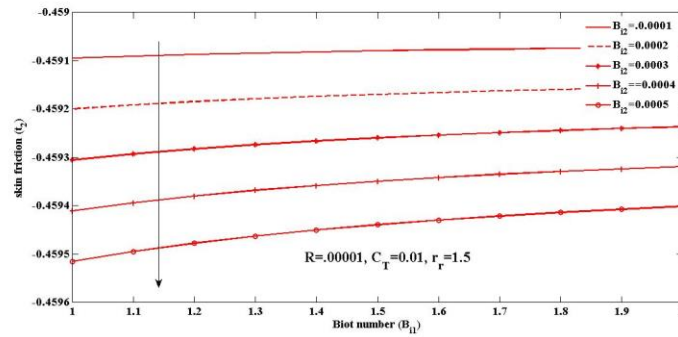


Figure 15: Skin friction profile at  $r = \lambda$  for different values of  $B_{12}$

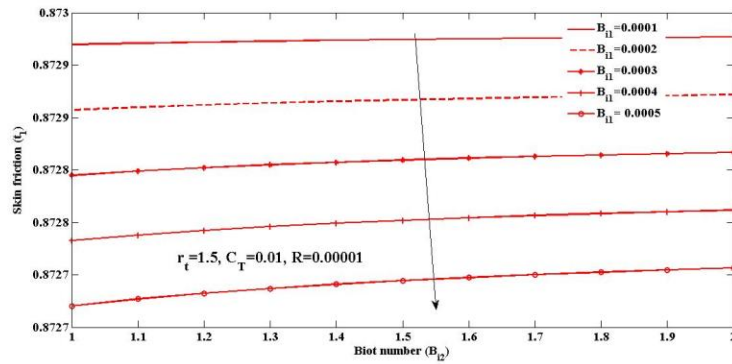


Figure 16: Skin friction profile at  $r = 1$  for different values of  $B_{i1}$

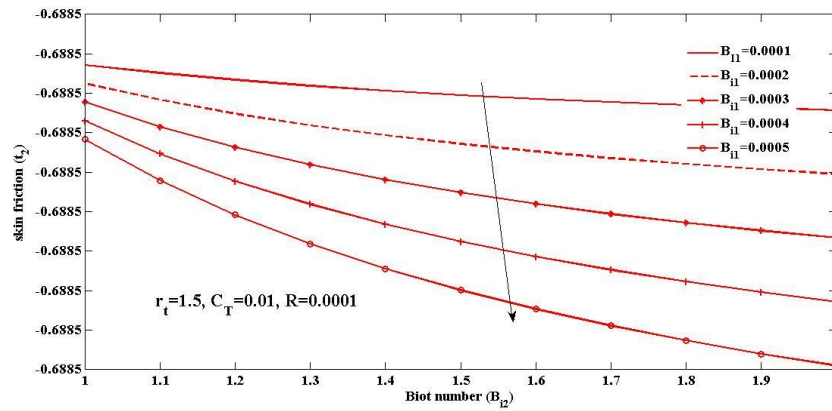
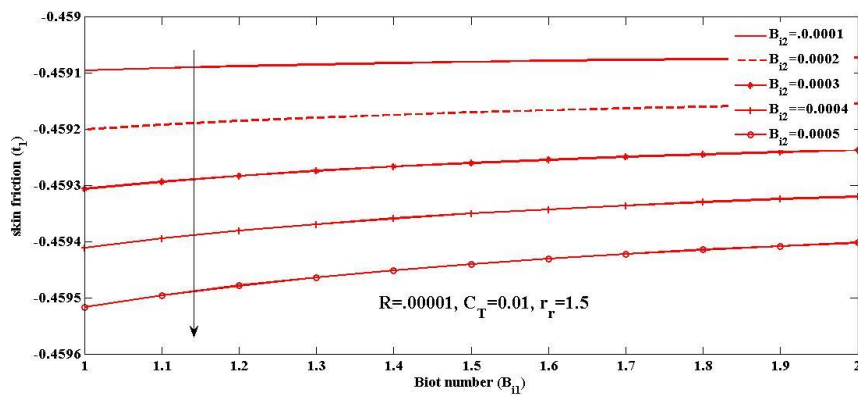


Figure 17: Skin friction profile at  $r = \lambda$  for different values of  $B_{i1}$



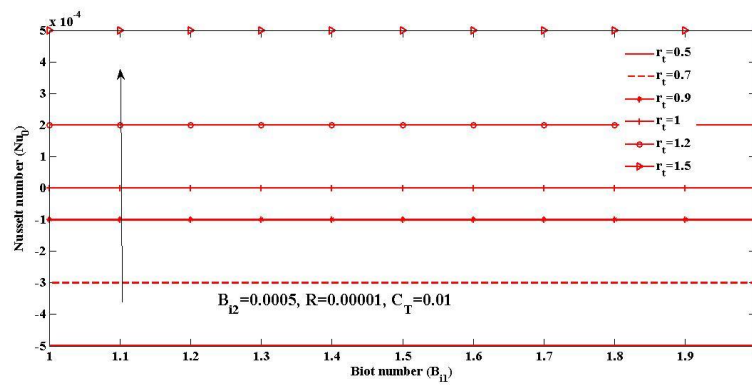


Figure 18: Nusselt number profile at  $r = 1$  for different values of  $r_t$

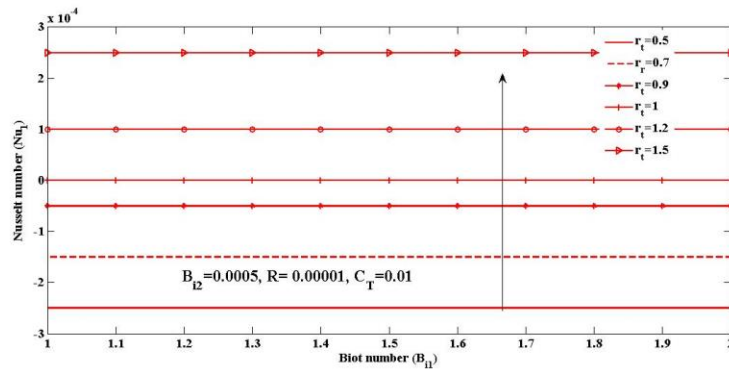


Figure 19: Nusselt number profile at  $r = \lambda$  for different values of  $r_t$

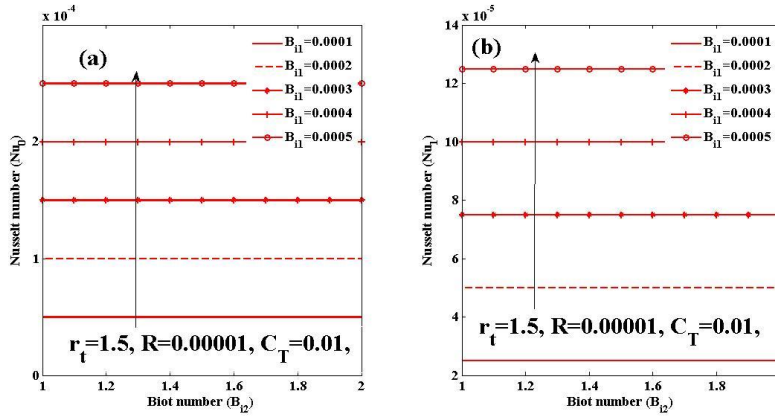


Figure 20: Nusselt number profile at  $r = 1$  and  $r = \lambda$  for different values of  $B_{12}$

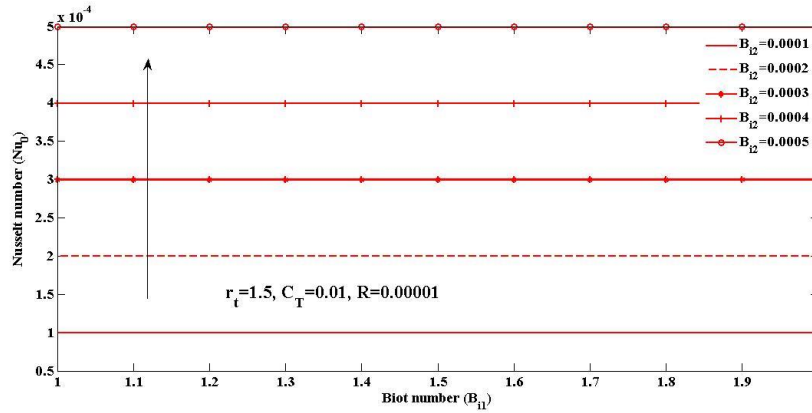


Figure 21: Nusselt number profile at  $r = 1$  for different values of  $B_{12}$

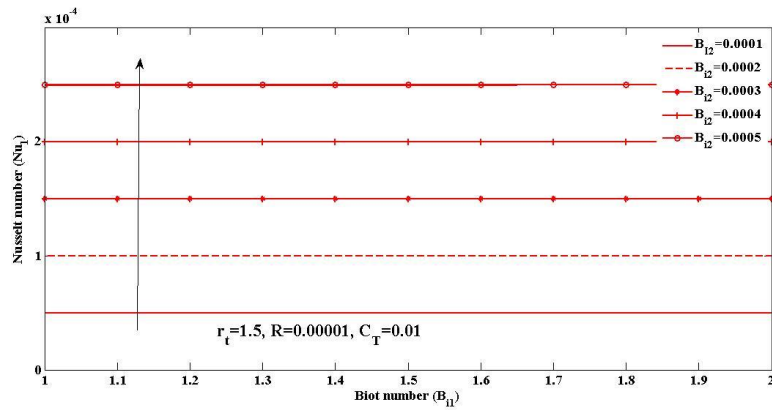


Figure 22: Nusselt number profile at  $r = \lambda$  for different values of  $B_{12}$

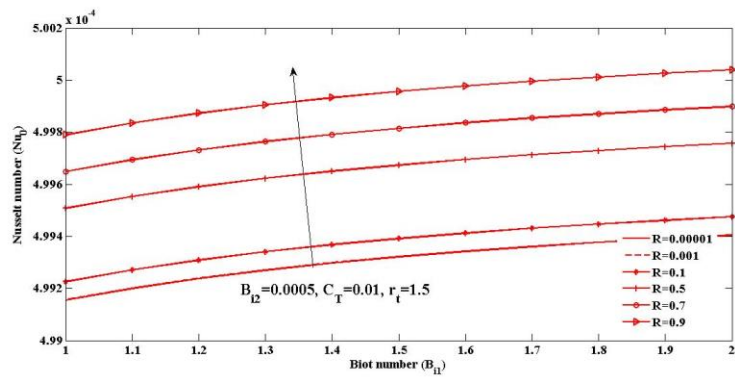
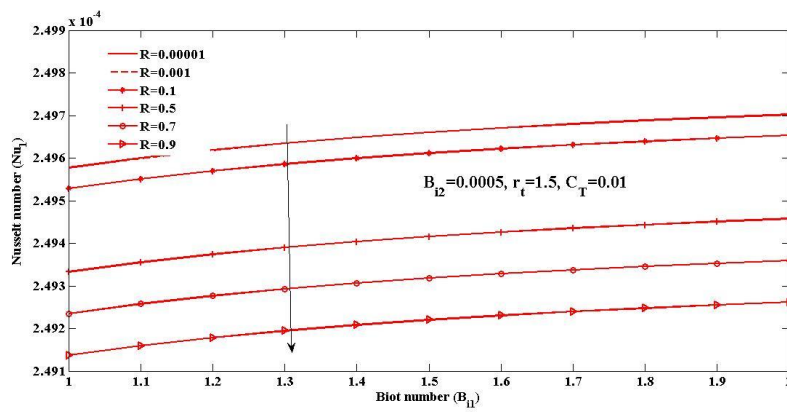


Figure 23: Nusselt number profile at  $r = 1$  for different values of  $R$



**Figure 24: Nusselt number profile at  $r = \lambda$  for different values of  $R$**

### 5.0 Discussion

The effects of the flow governing parameters on velocity, temperature, skin friction and Nusselt number, have been shown using line graph as shown from figure 2 to figure 24. These results show the variations in the velocity, temperature, skin friction, and Nusselt number, are influenced by the material parameters of the flow problem, that is, the radiation parameter ( $R$ ), temperature difference parameter ( $\tau_t$ ), Biot numbers ( $B_{i1}$  and  $B_{i2}$ ) and thermal diffusion parameter  $\tau_t$ . The radiation parameter  $R$  is in the range of  $0 \leq R \leq 1$  to avoid finite time temperature blow up (Makinde and Chinyoka 2010, Isah *et al* (2016)).

Figures 2-5 show velocity profile with different material parameters while figure 6 to figure 9 display the effect of the material parameters on the Temperature. Figure 10 to figure 17 describe the influence of the parameters on Skin friction while figure 18 to figure 24 show the effect of parameters on Nusselt number.

Figure 2 and figure 3 describe the effect of Biot numbers  $B_{i1}$  and  $B_{i2}$  respectively on velocity. It is seen that, increase in  $B_{i1}$  leads to increase in velocity while increase in  $B_{i2}$  leads to decrease in velocity. Figure 4 depicts the influence of thermal radiation parameter  $R$  on velocity. It shows that, increase in  $R$  has no significant effect on velocity. Figure 5 describes the effect of thermal diffusion parameter  $\tau_t$  on velocity. It shows that, increase in  $\tau_t$  leads to increase in velocity. Figure 6 describes the effect of Biot number  $B_{i1}$  on temperature. It shows that increase in  $B_{i1}$  leads to decrease in temperature. Figure 7 describes the influence of  $B_{i2}$  on temperature. It shows that an increase in  $B_{i2}$  leads to increase in temperature. Figure 8 describes the influence of  $\tau_t$  on temperature. It is seen that, increase in  $\tau_t$  leads to increase in temperature. Figure 9 depicts the effect of  $R$  on temperature. It shows that, increase in  $R$  leads to increase in temperature. Figure 10 describes the effect of  $\tau_t$  on skin friction at the outer surface of the inner cylinder ( $r = 1$ ). It shows that, increase in  $\tau_t$  leads to decrease in skin friction at  $r = 1$ . Figure 11 depicts the influence of  $\tau_t$  on skin friction at the inner surface of the outer cylinder ( $r = 2$ ). It shows that, increase in  $\tau_t$  leads to decrease in skin friction at  $r = 2$ . Figures 12 and 13 describe the influence of  $R$  on skin friction. It is seen that at both  $r = 1$  and  $r = 2$ , there is no effect on the skin friction as  $R$  changes. Figure 14 to figure 17 describe the effect of Biot numbers  $B_{i1}$  and  $B_{i2}$  on skin friction at  $r = 1$  and  $r = 2$ . Figures 14 and 15 show that, increase in Biot number  $B_{i2}$  leads to decrease in skin friction at both  $r = 1$  and  $r = 2$  respectively. Figures 16 and 17 show that, increase in the Biot number  $B_{i1}$  also leads to decrease in skin friction at both  $r = 1$  and  $r = 2$  respectively. Figures 18 and 19 describe the influence of  $\tau_t$  on Nusselt number. It shows that increase in  $\tau_t$  leads to increase in Nusselt number at both  $r = 1$  and  $r = 2$ . Figure 20 describes the influence of  $B_{i1}$  on Nusselt number. It shows that increase in  $B_{i1}$  leads to increase in Nusselt number at both  $r = 1$  and  $r = 2$ . Figures 21 and 22 describe the influence of  $B_{i2}$  on Nusselt number. It shows that increase in  $B_{i2}$  leads to



increase in Nusselt number at  $r = 1$  and  $r = 2$ . Figures 23 and 24 describe the influence of R on Nusselt number. It is seen that, increase in R leads to increase in Nusselt number at  $r = 1$ ; whereas increase in R leads to decrease in Nusselt number at  $r = 2$ .

## 6.0 Conclusions

Free-convective steady-state MHD flow restricted through an annulus with boundary condition of mixed kind has been discussed. From the above result, the following observations were made and concluded that:

1. Increase in Biot number  $B_{i1}$  leads to increase in velocity but decrease in temperature.
2. Increase in Biot number  $B_{i2}$  leads to decrease in velocity but increase in temperature.
3. Increase in thermal radiation parameter R leads to increase in temperature and this will consequently leads to increase in the velocity.
4. Increase in thermal diffusion parameter  $r_t$  leads to increase in velocity and temperature
5. Increase in thermal diffusion parameter  $r_t$  leads to decrease in skin friction at both outer surface of the inner cylinder and inner surface of the outer cylinder i.e. at  $r = 1$  and  $r = 2$
6. Increase in Biot numbers  $B_{i1}$  and  $B_{i2}$  lead to decrease in skin friction at both outer surface of the inner cylinder and inner surface of the outer cylinder i.e at  $r = 1$  and  $r = 2$
7. Increase in  $r_t$  leads to increase in Nusselt number at both  $r = 1$  and  $r = 2$
8. Increase in Biot numbers  $B_{i1}$  and  $B_{i2}$  lead to increase in Nusselt number at both  $r = 1$  and  $r = 2$
9. Increase in R leads to increase Nusselt number at  $r = 1$  but decrease at  $r = 2$

## References

1. Adachi, T. and Imai, S. (2007). "Three-Dimension Linear Stability of Natural Convection in Horizontal Concentric Annuli". *International Journal of Heat and Mass Transfer*, 50, 1388-1396.
2. Alawadi, E.M. (2008) "Natural Convection Flow in a Horizontal Annulus with an Oscillating . Inner Cylinder Using Lagrangian-Eulerian Kinematics". *Computers & Fluids*, 37, 1253-1261.
3. Ashorynejaeed, H.R., Mohamad, A.A. and Sheikholeslam, M. (2013) "Magnetic Field Effects on Natural Convection Flow of a Nano fluid in a Horizontal Cylindrical Annulus using Lattice Boltzmann Method". *International Journal of Thermal Sciences*, 64, 240-250.
4. Chen, H. and Hsu, W. (2007) "Estimation of Heat Transfer Coefficient on the Fin of Annular-Finned Tube Heat Exchangers in Natural Convection for Various Fin Spacing". *International Journal of Heat and Mass Transfer*, 50, 1750-1761.
5. Cienfrini, M., Corcione, M. and Quintino, A. (2011) "Natural Convection Heat Transfer of Nanofluids in Annular Spaces between Horizontal Concentric Cylinders". *Applied Thermal Engineering*, 31, 4055-4063.
6. Date, A.W. (1986) "Numerical Prediction of Natural Convection Heat Transfer in Horizontal Annulus". *International Journal of Heat and Mass Transfer*, 29, 1457-1464.

7. Habibi Matin, M. and Pop, I. (2013) "Effect of Natural Convection Flow and Heat Transfer in an Eccentric Annulus Filled by Copper Nano fluid". *International Journal of Heat and Mass Transfer*, 61, 353-364.
8. Ho, C.J., Lin, Y.H. and Chen, T.C. (1988) "A Numerical Study of Natural Convection in Concentric and Eccentric Horizontal Cylindrical Annuli with Mixed Boundary Conditions". *International Journal of Heat and Fluid Flow*, 10, 40-47.
9. Isah B.Y, Jha B.K. and Lin J.E. (2016) "Combined effect of Thermal Diffusion and Diffusion thermo effects on Transient MHD Natural convection and mass transfer flow in a vertical channel with thermal Radiation". *Journal of Applied Mathematics*, 7, 2354-2373.
10. Jeng, T., Tzeng, S. and Lin, C. (2007) "Heat Transfer Enhancement of Taylor- Couette-Poiseuille Flow in an Annulus by Mounting Longitudinal Ribs on the Rotating Inner Cylinder". *International Journal of Heat and Mass Transfer*, 50, 381-390.
11. Jha B.K., Yabo I.B. and Lin J. E. (2017) "Transient natural convection in an annulus with thermal radiation". *Journal of Applied Mathematics* 8, 1351-1366.
12. Kumar, R. (1988). "Study of Natural Convection in Horizontal Annuli". *International Journal of Heat and Mass Transfer*, 31, 1137-1148.
13. Makinde, O.D. and Chinyoka, T. (2010). "Numerical Investigation of Transient Heat Transfer to Hydromagnetics Channel Flow with Radiative Heat and Convective Cooling". *Communication in Nonlinear Science and Numerical Simulation*, 15, 3919-3930.
14. Mizushima, J., Hayashi, S. and Adachi, T. (2001) "Transitions of Natural Convection in a Horizontal Annulus." *International Journal of Heat and Mass Transfer*, 44, 1249-1257.
15. Shah, M., Mahmoudi, A.M. and Talebi, H. (2011). "A Numerical Investigation of Conjugate-Natural Convection Heat Transfer Enhancement of a Nanofluid an Annular Tube Driven by Inner Heat Generating Solid Cylinder". *International Communications in Heat and Mass Transfer*, 38, 533-542.
16. Sheikholeslami, M., Gorji-Bandpay, M., Ganji, D.D. and Soleimani, S. (2012). "Magnetic Field Effects on Natural Convection around a Horizontal Circular Cylinder inside a Square Enclosure Filled with Nano fluid". *International Communications in Heat and Mass Transfer*, 36, 978-986.
17. Sheikholeslami, M., Gorji-Bandpay, M., Ganji, D.D. and Soleimani, S. (2013). "Effect of Magnetic Field on Natural Convection in an Inclined Half-Annulus Enclosure Filled with Cu-Water Nano fluid using CVFEM". *Advanced Powder Technology*, 24, 980-991.
18. Shihhao Y, Tsai-jin C. and Jik C.L. (2014). "Analytical solution for MHD flow of a magnetic fluid with a thick porous annulus". *Journal of Applied Mathematics*, 2014 931732.
19. Soleimani, S., Sheikholeslami, M., Ganji, D.D. and Gorji-Bandapay, M. (2012). "Natural Convection Heat Transfer in a Nano fluid Filled Semi-Annulus Enclosure". *International Communications in Heat and Mass Transfer*, 39, 565-574.
20. Tahir, S. and Mital, M. (2012). "Numerical Investigation of Laminar Nanofluid Developing Flow and Heat Transfer in a Circular Channel". *Applied Thermal Engineering*, 39, 8-14.
21. Tsui, Y.T. and Tremblay, B. (2000). "On Transient Natural Convection Heat Transfer in the Annulus between Concentric, Horizontal Cylinder with Isothermal Surfaces". *International Journal of Heat and Mass Transfer*, 27, 103-111.
22. Yeh, C. (2002). "Numerical Investigation of the Three-Dimensional Natural Convection inside Horizontal Concentric Annulus with Specified Wall Temperature or Heat Flux". *International Journal of Heat and Mass Transfer*, 45, 775-784.
23. Yoo, J.-S. (2003). "Dual Free-Convection Flows in a Horizontal Annulus with a Constant Heat Flux Wall". *International Journal of Heat and Mass Transfer*, 46, 2499-2503.
24. Yoo, J.-S. (1998). "Natural Convection in a Narrow Horizontal Cylindrical Annulus:  $Pr \leq 0.3$ ". *International Journal of Heat and Mass Transfer*, 41, 3055-3073.

25. Yoo, J.-S. (1999). "Prandtl Number Effect on Bifurcation and Dual Solutions in Natural Convection in a Horizontal Annulus". *International Journal of Heat and Mass Transfer*, 42, 3279-3290.